



Universiteit
Leiden
The Netherlands

Regulation of target proteins by small ubiquitin-like modifiers

Xiao, Z.

Citation

Xiao, Z. (2019, June 5). *Regulation of target proteins by small ubiquitin-like modifiers*. Retrieved from <https://hdl.handle.net/1887/74009>

Version: Publisher's Version

License: [Licence agreement concerning inclusion of doctoral thesis in the Institutional Repository of the University of Leiden](#)

Downloaded from: <https://hdl.handle.net/1887/74009>

Note: To cite this publication please use the final published version (if applicable).

Cover Page



Universiteit Leiden



The following handle holds various files of this Leiden University dissertation:

<http://hdl.handle.net/1887/74009>

Author: Xiao, Z.

Title: Regulation of target proteins by small ubiquitin-like modifiers

Issue Date: 2019-06-05

Chapter 5

UFMylation: an emerging post-translational modification regulating protein synthesis

Katharina F. Witting^{1*}, Zhenyu Xiao^{1*}, Román González-Prieto¹, Huib Ovaa^{1, #}, Alfred C.O. Vertegaal^{1, #}

Affiliations: ¹Department of Cell and Chemical Biology, Division of Chemical Immunology, Leiden University Medical Center (LUMC), Einthovenweg 20, 2333 ZC, Leiden, The Netherlands

* These authors contributed equally

Address correspondence to: H.O. (h.ovaa@lumc.nl) and A.C.O.V. (e-mail: vertegaal@lumc.nl)

Summary

UFMylation is a reversible post-translational modification implicated in a variety of biological processes including ER homeostasis upon unfolded protein response (UPR), erythroid differentiation, and more recently coordinating interaction of mRNA and other proteins to the ribosome. We studied global UFMylation in a site-specific manner in both wildtype and UFSP2 knockout cells. We identified seven proteins (RPL26, RPL26L1, TUBA1B, MCM5, SLC26A7, SCYL2, WDR63) for which we could map the modified lysines. Interestingly, we found UFMylation of RPL26 (L24), a 60S ribosomal protein, that we demonstrate to specifically interact with the signal recognition particle receptor (SRPR). Together, these results shed a new light on the biological role of UFM1 and open new avenues of research to clarify the physiological role of the UFM1-system.

1 Introduction

Post-translational modifications (PTMs) tightly regulate protein functions either through the addition of chemical moieties like methylation, acetylation and phosphorylation or small protein modifiers that belong to the ubiquitin-like (Ubl) family to specific residues of their target proteins^{1,2}. Besides ubiquitin, other proteins such as Small Ubiquitin-like Modifiers (SUMOs), Atg8, Atg12, FUBI, FAT10, HUB1, ISG15, Nedd8, URM1 and UFM belong to the Ubl family^{3,4}. As a result of these PTMs, functional study on proteomics become extremely complex^{5,6}.

Phosphorylation and ubiquitination are the most common and well-studied post-translational modification mechanisms in eukaryotes⁷⁻⁹. Small ubiquitin-like modifiers (SUMOs), have also been extensively studied in the past two decades. Thousands of SUMO substrates as well as acceptor lysines were discovered by mass spectrometry (MS) analyses¹⁰⁻¹⁴, which provided a wealth of resources for further functional study of these modifications. However, only limited information is available about other Ubl conjugation systems such as UFM1.

UFM1, a recently identified ubiquitin-like protein, resembles ubiquitin, covalently modifies lysine residues of its substrates through a three components enzymatic cascade¹⁵⁻¹⁹. UFM1 is translated as an inactive precursor form (pro-UFM1) which has one or two additional amino acids beyond the conserved single glycine and are cleaved by UFSP2 to expose the UFM1- single active C-terminal glycine. Mature UFM1 is activated as an adenylate by UBA5 forming a high-energy thioester bond with the active-site cysteine of UBA5. This allows the transfer onto the catalytic site of the E2 enzyme-UFC1, where again a thioester bond is formed. With the action of the E3-like enzyme, UFL1, activated UFM1 is transferred onto the lysine residues of the protein substrates, forming an isopeptide bond. Similar to ubiquitin, UFMylation is reversed by cleavage of UFM1 specific protease, UFSP2. UFM1 has six lysines which are amenable to forming poly-UFMylation^{20,21}.

The main conserved function of the ribosome is translation of the genomic code into proteins^{22,23}. The eukaryotic ribosome consists of 80 ribosomal proteins and a ribosomal RNA shell^{24,25}. Secretory proteins are delivered through the secretory pathway. In this pathway proteins possessing signal sequences are recognized at the ribosome by the signal recognition particle (SRP) while they are still undergoing synthesis. With the help of SRP and its membrane bound receptor (SRPR or SR), co-translational secretory and membrane proteins are directly translocated into the translocation channel and finally into the ER²⁶.

UFMylation has been connected to biological processes including ER homeostasis, vesicle trafficking, autophagy and more recently it has been demonstrated to modify ribosomal proteins^{27, 29,30}. A failure to conjugate UFM1 to target proteins results in the promotion of tumor formation²⁰. Loss of function of UFMylation in mice leads to apoptosis in fetal liver cells and pancreatic beta cells²¹. Using an improved immunoprecipitation approach, Simsiek et al. reported UFMylation of a ribosomal protein (eL36) and its interaction with the UFM1 E3 ligase UFL1²⁷. More recently, Pirone et al reported their

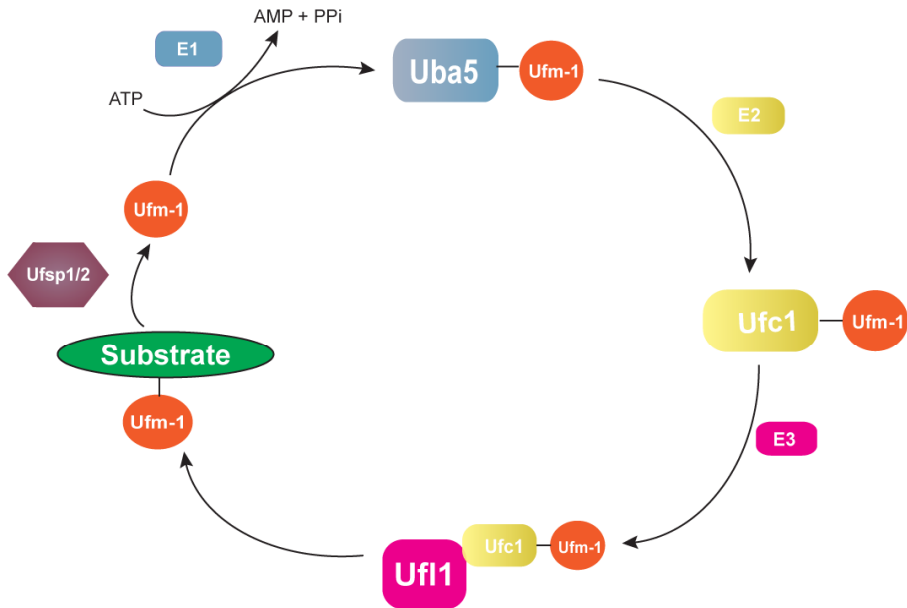
identification of 494 UFMylated proteins, of which 82 survived stringent filtering²⁸. However, none of them been independently validated and no biological function studies have been well conducted to elucidate the role of protein UFMylation. Despite these interesting findings, the biological consequences of UFMylation remain obscure.

Given the lack of understanding of biological processes involving UFMylation, as well as the transient nature of UFM1 modification, substrate identification has posed major technical challenges and urgently calls for the development of proteomics methods. To address this problem, we adapted the mass spec technology developed by Hendriks et al^{10,13}. by combining it with CRISPR/Cas9-mediated gene knockout of the only known UFM1 specific protease-UFSP2 that is active in mammalian cells, to enrich UFMylated substrates and to identify UFM1 specific acceptor lysines. Seven proteins with UFM1 acceptor lysines have been identified in our screen. One of the major UFM1 modified proteins was the ribosomal protein RPL26. We found that UFMylated RPL26 can efficiently interact with signal recognition particle receptor (SRPR). Our findings provide new insight in UFM1 signal transduction.

2 Results

UFM1 is a 9.1-kDa protein with a similar tertiary structure to ubiquitin and with a similar three component enzymatic cascade. Mature UFM1 can be attached to target proteins. Deconjugation of UFM1 is mediated by the two UFM1-specific proteases, UFSP1 and UFSP2 (**Figure 1 A and B**). Previously Ishimura et al. has shown that knockdown of UFSP2 leads to an increase in UFMylation, thereby enabling the enrichment of UFM1 modified proteins³¹. We employed CRISPR-Cas9 mediated genome editing to knock out UFSP2 in HeLa cells (**Figure 2A**).

A



B Alignment of Ufm1 and Ub

```

sp|P61960|UFM1  MS---KVSFKITLTSDFRLPYKVLSPVESTPFATLKFAAEEFKVFAATSATITNDGIGINPAQTAGNVFLKHGRELRTIPDRVGVSC
sp|P0CG48|UBC  MGIFVKTLTGKTLTLEVEFSD-----TIENKAKIQDKEGIFDDQRIIFAKKQLEDGRITLSDQYNQKHEITLHLVLLRGL--

```

Figure 1. UFM-1 cascade and UFM-1. A) Ufm-1 conjugation machinery B) UFM-1 sequence alignment with Ubiquitin (Ub) shows that the C-terminal di-glycine motif characteristic of Ub is replaced by a valine- glycine motif in UFM-1.

2.1 Proteomics approach to study global UFMylation in UFSP2 knockout cells

Given that the knockout of UFSP2 in HeLa cells caused a significant increase in overall UFMylation and slightly decreased cell proliferation, we were interested in identifying UFM1 target proteins as well as acceptor lysines in UFSP2 knock out cells using a proteomics approach. Due to the nature of UFM1, one major challenge in addressing this is that analogous technologies used for identification of ubiquitinated substrates (e.g. di-Gly proteomics) are unavailable for UFM1, as antibodies targeting VG-sites are still not available. Furthermore, the abundance of UFMylated proteins is magnitudes lower than that of ubiquitination or SUMOylation, posing a major challenge for proteomics³².

To address this, we have adapted the biochemical purification of SUMO target proteins and SUMO sites developed by Hendriks et al¹⁰. We generated a HeLa cell line and a HeLa cell line with UFSP2 knockout stably expressing a His10-tagged lysine-deficient UFM1 (His10-UFM1-K0) to enable UFM1 acceptor lysine mapping (**Figure 2B**). To generate a stable cell line, we used puromycin as marker

for selection. Immunoblot analysis confirmed the slightly increased expression of His10-UFM1-K0 compared with endogenous levels of UFM1 in HeLa cells and the efficient purification of UFM1 conjugates by the His10-UFM1-K0 method (**Figure 2 C and D**).

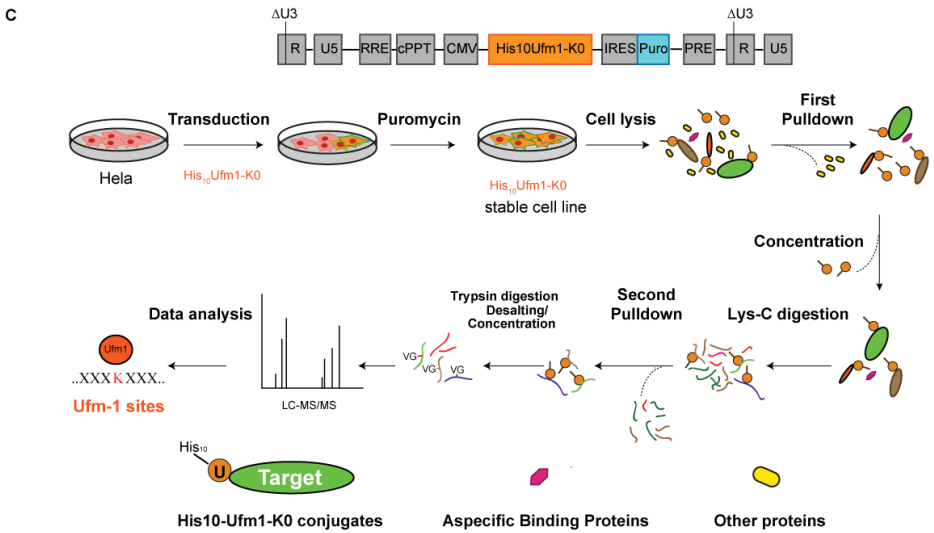
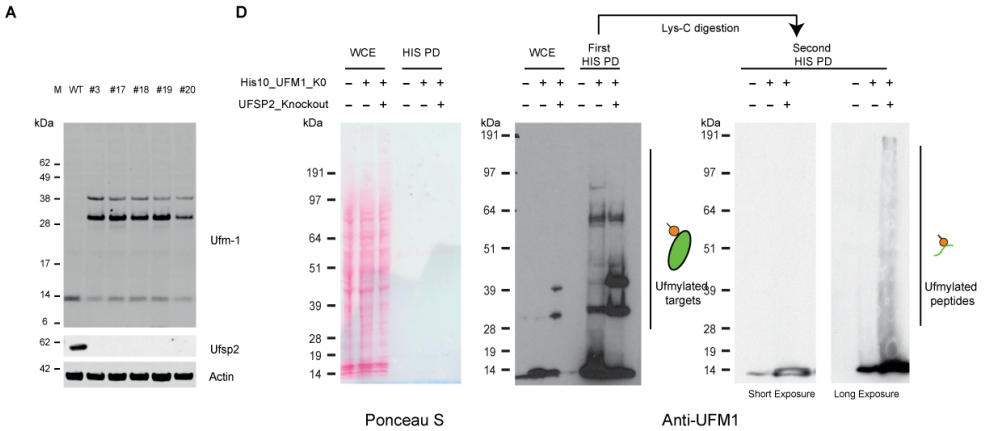


Figure 2. Generation and validation of HeLa cells stably expressing His10-UFM1-K0 with or without UFSP2. **A)** UFSP2 depletion increases UFMylation. UFSP2 was knocked out using CRISPR-CAS9 gene editing technology. The efficiency of UFSP2 knock out was assessed by immunoblotting using an antibody against UFSP2. Depletion of UFSP2 caused an increase of UFMylation as shown by immunoblotting using an antibody against UFM1. **B)** Sequence of His10-UFM1-K0 protein used to generate stable cell lines in either HeLa or HeLa UFSP2 knockout cells. **C)** Cartoon depicting the strategy to identify UFM1 targets as well as acceptor lysines. **D)** Purification of His10-UFM1-K0 conjugates via NTA purification was confirmed by immunoblotting. Whole cell extracts and UFM1 purified proteins of cells were run on 4-12% Bis-Tris polyacrylamide gels and levels of His10-UFM1 conjugates were compared by immunoblotting using anti-UFM1 antibody. Ponceau-S staining was performed to confirm the purity of the final fraction.

We used this cell line to enrich and purify UFMylation peptides from HeLa cells (His10-UFM1-K0) or HeLa cells (His10-UFM1-K0) without UFSP2. Wild type HeLa cells were used as the negative control. Cells were cultured using a lower puromycin concentration to ensure stable expression. To enrich the His10-UFM1 modified proteins, a two-step purification strategy was employed as described in Figure 2 C¹⁰. For proteomic analysis, three biological replicates with two technical repeats for all cell lines were analyzed in this study. In total, 13 sites were identified in seven proteins, which are RPL26, RPL26L1, TUBA1B, MCM5, SLC26A7, SCYL2, WDR63 (**Figure 3A**).

2.2 RPL26 is extensively UFMylated

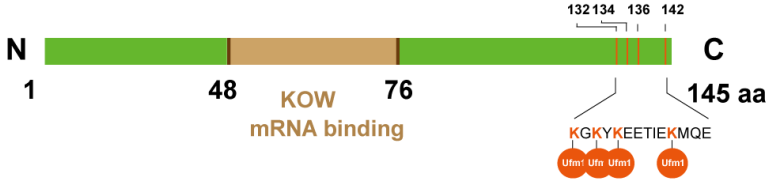
The ribosome production is a fundamental process in cell biology. RPL26 overexpression inhibits cell proliferation and induces cell cycle arrest through activating p53³³ and later more studies indicated that RPL26 controls p53 protein levels through binding to the 5' untranslated region of the p53 mRNA³⁴. However, little is known about its post translational modifications and its role in protein synthesis. We selected RPL26 for further validation to study its regulation by UFMylation because it is the top UFM1 target identified in our screen.

We found four UFM1 acceptor lysines in the C-terminus of RPL26 (K132, K134, K136 and K142) (**Figure 3 A and B**). Interestingly, alignment of orthologous genes showed that these four acceptor lysines are highly conserved across species probably due to their functional importance (**Figure 3C**). Immunoblotting analysis of endogenous RPL26 and Flag-RPL26 in His10-UFM1-K0 HeLa cells and UFSP2 knockout HeLa cells revealed that UFMylation of RPL26 strongly increased in the absence of UFSP2 (**Figure 3 D and E**). Increased RPL26-UFMylation thus can be explained by depletion of UFSP2.

A

Protein names	VG (UFM1) site within proteins	VG (UFM1) site positions	Score
RPL26 / RPL26L1	132	KILERKAKSRQVGKEK KG YKEETIEKMQE__	210.35/140.14
RPL26 / RPL26L1	134	LERKAKSRQVGKEK KG YKEETIEKMQE__	100.22/62.16
RPL26 / RPL26L1	136	RKAKSRQVGKEK KG YKEETIEKMQE__	69.03/60.16
RPL26	142	QVGKEK KG YKEETIEKMQE__	64.84
TUBA1B	370	INYPPTVPGGDLAK V QRAVCMLSNTAIA	92.93
MCM5	582	VRQLEAIVRIEALSK M KLQPFATEADVEEA	61.16
SLC26A7	120	SIVLLVLVKELNEQ F RKIVKVLVPLDVLUI	60.91
SCYL2	73	KQEVAVFVDK L DK Y QKFEKDQIDSLKR	59.91
SCYL2	76	VAVFVFDK L DK Y Q F EKDQIDSLKRQV	59.91
WDR63	564	DHLGK T GQK M LAG S K T EKAEMMP Y HN L ES	45.28

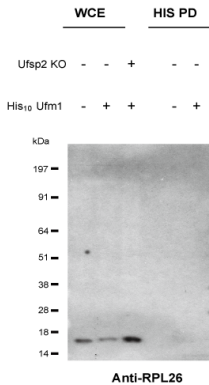
B



C

	10	20	30	40	50	60	70
RPL26_YEAST1-127	MAKQSLDVSSDRR	KARKAYFTAPSSQRRVLLSAPLSKELRAQYV	IKALPIRRDDEVLVVRGSKKGQEGK	ISSVY			
Q9VUJ2_DROME1-149	MKNPNFVTSRRR	KNRKRFNAPSHIRRLMSAPLSKELRQKYNVRSMP	IRRDDEVQVIRGFHKGQVQKVVQAY				
RPL26_MOUSE1-145	MKFNPFVTSDRS	KNRKRFNAPSHIRRKIMSSPLSKELRQKYNVRSMP	IRKDDDEVQVVRGHYKGGQ	IGKVVQVY			
RPL26_HUMAN1-145	MKFNPFVTSDRS	KNRKRFNAPSHIRRKIMSSPLSKELRQKYNVRSMP	IRKDDDEVQVVRGHYKGGQ	IGKVVQVY			
RPL26RAT1-145	MKFNPFVTSDRS	KNRKRFNAPSHIRRKIMSSPLSKELRQKYNVRSMP	IRKDDDEVQVVRGHYKGGQ	IGKVVQVY			
H2QC81_PANTR1-145	MKFNPFVTSDRS	KNRKRFNAPSHIRRKIMSSPLSKELRQKYNVRSMP	IRKDDDEVQVVRGHYKGGQ	IGKVVQVY			
RPL26_CAEEL1-145	MKVNPFVSSDS	SGSKRKAHFNAPSHERRRIMSAPLTKELRTKHG	IRAIPIRTDDEVVVMRGRHKGNTGRVLR	RCYR			
F7F4S1_MACMU1-145	MKFNPFVTSDRS	KNRKRFNAPSHIRRKIMSSPLSKELRQKYNVRSMP	IRKDDDEVQVVRGHYKGGQ	IGKVVQVY			
Q75XA1_DANRE1-145	MKLNFTVTSRRR	KNRKRFNAPSHIRRKIMSSPLSKELRQKYNVRSMP	IRKDDDEVQVVRGHYKGGQ	IGKVVQVY			
RPL26_SCHPO1-126	MKFSRDVTSRRR	KQRKAHFGAPSSVRRVLSAPLSKELREQYK	IRSLPVRDDQITVIRGSKNGREGKIT	TSVYR			
	80	90	100	110	120	130	140
RPL26_YEAST1-127	RLKFAVQDKVTKE	KVNGASVPIINLHPSKLVITKHLDKDRKAL	IQRKGGKLE---				
Q9VUJ2_DROME1-149	RKFFVYVVEKIQ	REANAGTNVVYGIHPSKVIIVKLLDKDRKAL	LERRGKRLAAL KG YKEETIEA	AQPMETA			
RPL26_MOUSE1-145	RKKYVIYIERVQ	REKANGTTVHVGIRPSKVVITRLKLDKDRKK	ILERKAKSRQVGKE KG YKEETIE	KMQE---			
RPL26_HUMAN1-145	RKKYVIYIERVQ	REKANGTTVHVGIRPSKVVITRLKLDKDRKK	ILERKAKSRQVGKE KG YKEETIE	KMQE---			
RPL26RAT1-145	RKKYVIYIERVQ	REKANGTTVHVGIRPSKVVITRLKLDKDRKK	ILERKAKSRQVGKE KG YKEETIE	KMQE---			
H2QC81_PANTR1-145	RKKYVIYIERVQ	REKANGTTVHVGIRPSKVVITRLKLDKDRKK	ILERKAKSRQVGKE KG YKEETIE	KMQE---			
RPL26_CAEEL1-145	-KFFVIHIDKI	TREKANGSTVHIGIHPKVAITRLKLDKDRRAL	VERKAAGRSRVGT IK GGKHTDET	VN---			
F7F4S1_MACMU1-145	RKKYVIYIERVQ	REKANGTTVHVGIRPSKVVITRLKLDKDRKK	ILERKAKSRQVGKE KG YKEETIE	KMQE---			
Q75XA1_DANRE1-145	RKKYVIYIERVQ	REKANGTTVHVGIRPSKVVITRLKLDKDRKK	ILERKAKSRQD IK EG KG YKEETIE	KMQE---			
RPL26_SCHPO1-126	KKFLLLIERV	REKANGASAVGIDASKVVIITKHLDKDRKDL	IVRRKGGKVE---				

D



E

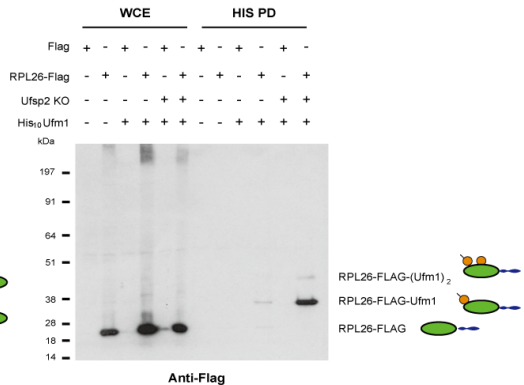
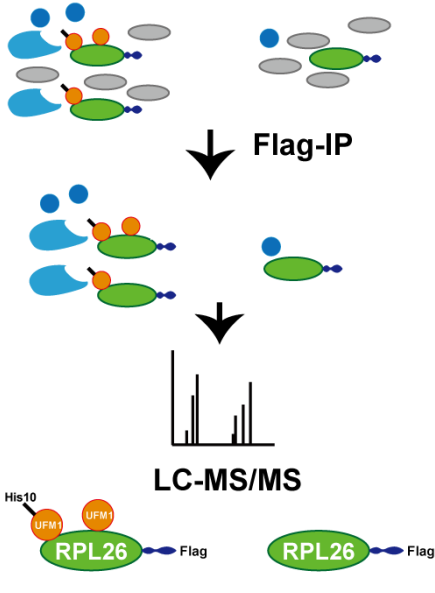


Figure 3. Label Free Quantification Results. **A)** VG-sites identified for UFM1 modified proteins by mass spectrometry. **B)** Domain structure of RPL26 highlighting the C-terminal UFM1 modification. **C)** Sequence Alignment of RPL26 reveals that the C-terminal lysine residues of this ribosomal protein are conserved across species except for yeast. **D)** HeLa cells with His10-UFM1-K0 and with or without UFSP2 were lysed and proteins were subjected to NTA purification. Whole cell extracts and UFM1 purified samples were analysed by immunoblotting using an antibody against RPL26. **E)** Flag-RPL26 was overexpressed in His10-UFM-K0 cell lines with or without UFSP2. Cells were lysed and proteins subjected to NTA purification. Whole cell extracts and UFM1 purified samples were analysed by immunoblotting using antibody against Flag.

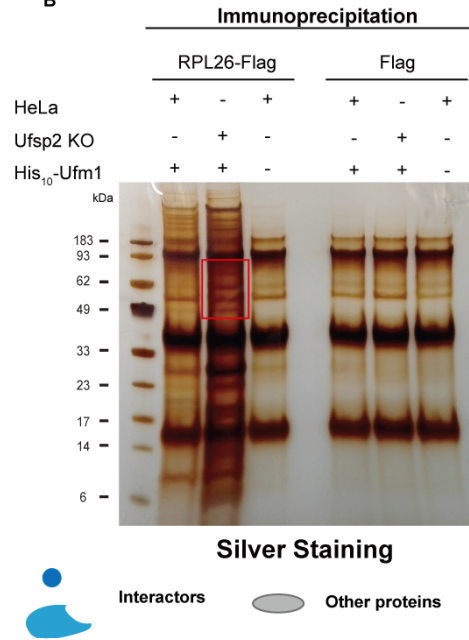
2.3 UFMylated RPL26 can directly interact with SRPR

Next, we asked whether UFMylation of RPL26 affected ribosome associated protein interaction. To investigate such protein interactions, we performed immunoprecipitation of ribosomes with modified or unmodified RPL26 coupled with a label free quantitative proteomics approach to identify proteins preferentially binding to UFMylated RPL26. In this case, Flag-RPL26 was transiently overexpressed in both HeLa cells and HeLa cells UFSP2 knockout cells stably expressing His10-UFM1-K0 and immunoprecipitated using an anti-Flag antibody. Proteins were digested on beads with trypsin and four independent experiments were performed (**Figure 4A**). Proteins were identified by mass spectrometry and silver staining were performed to confirm the purity of the final fraction (**Figure 4B**). Volcano plots shown in Figure 4C indicate the proteins preferentially binding to UFMylated RPL26.

A



B



C

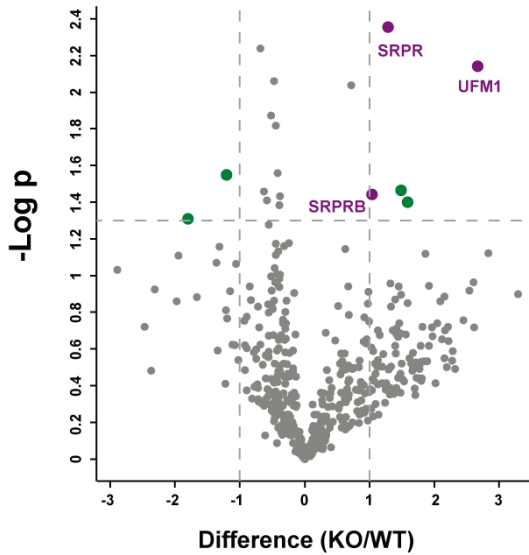


Figure 4. RPL26-UFMylation alters the interaction of ribosome associated proteins. **A)** Cartoon depicting the strategy to identify interactors of UFMylation of RPL26. **B)** Silver staining of mass spec samples. Co-Immunoprecipitation of Flag-RPL26 from either the wild type or the UFSP2 knockout HeLa cells stably expressing His10-UFM-K0. The silver stained gels reveal that there are indeed differences between the modified and the unmodified RPL26 containing ribosomes. **C)** Volcano plots showing proteins preferentially binding to UFMylation of RPL26.

Most notably, the signal recognition particle alpha (SRPR) interacts with UFM1 modified ribosomes in the UFSP2 KO His10-UFM1-K0 cells, but less when UFM1 is removed by the UFSP2 protease. This interaction could be confirmed by co-immunoprecipitation, which clearly showed that the UFM1 modified ribosome preferentially interacts with SRPR (**Figure 5 A and B**).

3 Discussion

It has been found that UFMylation is important to promote interactions between proteins¹⁵. Only little is known about the target proteins regulated by UFM1^{20,27,28,35}. To identify UFM1 target proteins as well as acceptor lysines, we have adopted a pioneering and well-developed method that has been proven to enable identification of SUMO acceptor lysines¹³. As a result, we successfully identified 8 novel UFM1 target proteins with 23 sites including RPL26 as a major UFM1 target in the absence of UFSP2. We confirmed RPL26 as a key UFM1 target and further confirmed that the UFMylation of RPL26 can efficiently interact with SRPR. Functional analysis of RPL26 such as RNA profiling of UFSP2 knockout HeLa cells revealed a role for UFM1-modified RPL26 in promoting translation elongation (data not shown).

3.1 PTM of ribosomal proteins

The mammalian ribosomes are composed of two subunits: 40S (small) and 60S (large) subunits. The 40S subunit is composed of 33 proteins and 18S rRNA, whereas the 60S subunit contains 46 proteins and three rRNAs (5S, 5.8S and 28S). While the 40S subunit is involved in the decoding of mRNA, the 60S subunit is responsible for peptide bond formation and export of nascent peptides^{22-24,36-41}. The rim of the exit point is composed of RNA, and a ring of four ubiquitously conserved ribosomal proteins (L22, L23, L24 and L29). L24 is RPL26^{42,43}. (**Supplementary Table 1**)

Among all ribosomal proteins, RPS6 is the first reported and best characterized phosphorylated ribosomal protein which is involved in PI3K, mTOR and Ras signalling pathways^{30,44,45}. Later, mouse models linked phosphorylation of RPS6 to the initiation of pancreatic cancer, however the physiological roles are still elusive⁴⁶. Another PTM modifying ribosomal protein is ubiquitin, which forms K63-linked chains on the RPL28/uL15 protein in yeast⁴⁷. Proteomic analysis of cells with chemically induced unfolded protein stress (UPR), revealed that mono-ubiquitination of small ribosomal proteins Rps2/uS5 and Rps3/uS3 was altered dynamically, most likely affecting protein-protein interaction⁴⁸. Using an improved immunoprecipitation approach, Simsiek et al. first report UFMylation of a

ribosomal protein (eL36) and its interaction with the UFM1 E3 ligase UFL1. However, they did not further investigate its biological impact on protein translation or protein-protein interaction²⁷.

3.2 UFMylation of RPL26 stimulates its interaction with SRPR.

Synthesis of new proteins is a very complex process. During translation of mRNA transcripts, various factors including enzymes and chaperones are involved in the processing, folding and targeting of nascent peptide chains to translocation pores at membranes⁴⁹. The ribosome plays a key role in these different tasks and serves as a platform for the regulated enzymes, targeting factors and chaperones that work on the newly translated polypeptides emerging from the exit tunnel. Secretory proteins are translated with an N-terminal signal sequence that can be recognized by the signal recognition particle (SRP). In order to target the ribosome-nascent chain complex to the endoplasmic reticulum membrane, SRP contacts the SRP receptor (SRPR) and leads the nascent chain transformation from the SRP into the lumen of the ER.

We immunoprecipitated ribosomes with modified or unmodified RPL26 coupled with a label free quantitative proteomics approach in order to identify associated factors. We identified the signal recognition particle receptor alpha (SRPR), to be significantly enriched in UFM1 KO cells, suggesting that this protein might be preferentially regulated by UFMylated RPL26. As expected, immunoblot analysis revealed that SRPR coimmunoprecipitated more efficiently with UFMylated RPL26 than with the non-UFMylated RPL26. These results suggest that the ribosome contacts the SRPR directly in the presence of UFM1 modification of RPL26 and does not require the signal recognition particle (SRP) to mediate the interaction. Upon examination of literature⁵⁰, the scenario seems to be the case, during the “handover” state of the ribosome, that is when the ribosome has been properly positioned over the SEC translocon and the SRP is being displaced. Taking our results into consideration, we hypothesize that UFM1 seems to mediate direct contact of the tunnel exit of the ribosome with the SRPR during the last step of direct peptides to the Sec61 translocon (**Figure 5C**). Our data indicate that RPL26 is one of the UFM1 target proteins serving as a platform for ribosome associated protein interaction.

The observation that SRPR can preferentially interact with UFMylated RPL26 in our experiments further raises the question how UFMylation specifically regulates translation. Given the novelty of this discovery, more experiments addressing the functional consequences on translation need to be performed to fully understand the role of UFM1 in this context. To answer this question, more studies are being performed (i.e. ribosome profiling, data not shown).

4 Conclusion

In this study, we identified seven proteins (RPL26, RPL26L1, TUBA1B, MCM5, SLC26A7, SCYL2, WDR63) that are covalently modified by UFM1. We describe for the first time a novel mechanism by which UFMylation might regulate proteins during the last step of the translation (elongation), after (or shortly before) the SRP leaves the ribosome and the ribosome correctly binds to the Sec61 translocon. The identification of the ribosomal protein RPL26 being modified by UFM1 might help to understand how UFM1 regulates protein synthesis by coordinating its targets.

5 Experimental procedures

Antibodies

The primary antibodies used for this study are: anti-UFSP2 (Abcam ab185965), anti-Actin (Sigma Aldrich A5941, Clone AC-15, ascites fluid), anti-UFM1 (Abcam ab109305), anti-RPL26 (Thermo Fisher Scientific, PA5-17093), anti-Flag (Sigma Aldrich, M2), anti-SRPR (Abnova H00006734-B02P). Secondary antibodies used for this study are: anti-mouse-800 (1: 10000 dilution; LiCOR, 926-3210) and anti-rabbit-800 (1: 10000 dilution; LiCOR, 926-3211). Fluorescent second antibody were used for visualization of labeled proteins on LICOR Odyssey system v3.0.

For immunofluorescence, goat anti-rabbit and goat anti-mouse AlexaFluor-488/568 conjugates (Thermo Fisher Scientific) were used.

Cloning, cell culture and cell line generation

The His10-UFM1-K0 we described and used in this manuscript has the following amino acid sequence:

MHHHHHHHHHHGGMSRVSFRITLTS DPRLPYRVLSVPESTPFTAVLRFAAEEFRVPAA
TSAIITNDGIGINPAQTAGNVFLRHGSELRIIPDRVG.

The corresponding nucleotide sequence was cloned in plasmid pLV-CMV-IRES-puro⁵¹. HeLa cell lines originated from ATCC, they were cultured under standard conditions (DMEM (Gibco) supplemented with 10% FCS (Sigma-Aldrich) at 37 °C with 5% CO₂). HeLa cells at 60% confluency were infected using a bicistronic lentivirus at an MOI of 3 encoding His10_UFM1_K0_IRES_puro. Following infection, cells were cultured under standard conditions as described before for two weeks under puromycin selection (2.5 μM). All cell lines used in this study were tested for mycoplasma contamination routinely with consistently negative outcome.

CRISPR-Cas mediated gene editing

UFSP2 guide RNA (gRNA) was designed using the CRISPR Design tool (<http://crispr.mit.edu/>), subcloned into a pX260 vector (Addgene).

UFSP2 guide RNA was subcloned into pX330-U6-Chimeric_BB-CBh-hSpCas9 (Addgene #42230, Cambridge, MA, USA), a human codon-optimized SpCas9 and chimeric guide RNA expression plasmid. CRISPR-mediated UFSP2 depletion in HeLa cells was performed by co-transfecting confluent HeLa with a vector harbouring the gRNA and the Cas9 and a construct conferring blasticidin resistance. After blasticidin selection and clonal expansion, UFSP2 depletion was verified by immunoblotting against using anti-UFSP2 antibody (1:1000 dilution, Abcam ab185965).

Electrophoresis and immunoblotting

Whole cell extracts or purified protein samples were separated on Novex Bolt 4-12% Bis-Tris Plus gradient gels (Life Technologies) using MOPS buffer or standard SDS-PAGE using a Tris-glycine

buffer and transferred onto Hybond-C nitrocellulose membranes (GE Healthcare Life Sciences) using a submarine system (Life Technologies). Membranes were stained with Ponceau S (Sigma) to visualize total protein amounts and subsequently blocked with 8% milk in PBS containing 0.05% Tween-20 before incubating with the primary antibodies as indicated.

Silver staining

For silver staining, gels were stained as described before⁵². Gels were incubated in Fixer (30% ethanol, 10% acetic acid) for 30 minutes and then washed two times in 20% ethanol and two times in water, 10 minutes each. Gels were sensitized in 0.8mM sodium thiosulfate for one minute and then rinsed in water twice for one minutes. Gels were then impregnated with 12 mM silver nitrate for 20 minutes and transferred to stop solution (40g of Tris and 20 ml of acetic acid per liter) for 30 minutes. Gels were then washed twice in water for 30 minutes.

Co-immunoprecipitation

For co-immunoprecipitation of RPL26-FLAG with endogenous interacting proteins, both HeLa cell lines stably expressing His10-UFM1 were transiently transfected with RPL26-FLAG or FLAG only as a background control. Cells were scraped on ice into ice cold co-immunoprecipitation buffer (50mM tris-HCl, pH 7.5, 1.5mM MgCl₂, 0.5% NP-40 and 5% Glycerol supplemented with 1mM DTT and a Complete Protease Inhibitor Tablet (Roche)). Lysates were clarified by centrifugation (4000rpm, 4°C, 20 min) and immunoprecipitated for 1h at 4°C with 3 µg Flag antibody followed by a 3h incubation with pre-equilibrated Protein-G Sepharose beads (GE Healthcare) at 4°C while rotating. After immunoprecipitation, samples were washed four times with ice-cold co-immunoprecipitation buffer and processed further for mass spectrometric analysis.

Purification of His10-UFM1 conjugates

Hela cells expressing His10-UFM1-K0 were washed, and scraped into ice-cold PBS. For total lysates, a small aliquot of cells was kept separately and lysed in 2% SDS, 1% N-P40, 50 mM TRIS pH 7.5, 150 mM NaCl. The remaining parts of the cell pellets were lysed in 6 M guanidine-HCl pH 8.0 (6 M guanidine-HCl, 0.1 M Na₂HPO₄/NaH₂PO₄, 10 mM TRIS, pH 8.0). The samples were snap frozen using liquid nitrogen, and stored at -80°C.

For His10-UFM1-K0 purification, the cell lysates were first thawed at room temperature and sonicated for 5 sec using a sonicator (Misonix Sonicator 3000) at 30 Watts to homogenize the lysate. Protein concentrations were determined using the bicinchoninic acid (BCA) protein assay reagent (Thermo Scientific) and lysate concentrations were equalized. Subsequently, imidazole as well as β-mercaptoethanol were added to a final concentration of 50 mM and 5 mM, respectively. His10-UFM1-K0 conjugates were enriched on nickel-nitrilotriacetic acid-agarose beads (Ni-NTA) (Qiagen), followed by washes with the following buffers A-D: Wash buffer A: 6 M guanidine-HCl, 0.1 M

Na₂HPO₄/NaH₂PO₄ pH 8.0, 0.01 M Tris-HCl pH 8.0, 10 mM imidazole pH 8.0, 5 mM β-mercaptoethanol, 0.1% Triton X-100. Wash buffer B: 8 M urea, 0.1 M Na₂HPO₄/NaH₂PO₄ pH 8.0, 0.01 M Tris-HCl pH 8.0, 10 mM imidazole pH 8.0, 5 mM β-mercaptoethanol, 0.1% Triton X-100. Wash buffer C: 8 M urea, 0.1 M Na₂HPO₄/NaH₂PO₄ pH 6.3, 0.01 M Tris-HCl pH 6.3, 10 mM imidazole pH 7.0, 5 mM β-mercaptoethanol, no Triton X-100. Wash buffer D: 8 M urea, 0.1 M Na₂HPO₄/NaH₂PO₄ pH 6.3, 0.01 M Tris-HCl, pH 6.3, 5 mM β-mercaptoethanol. For samples subjected to immunoblotting, wash buffers containing 0.2% Triton X-100, were used. Samples were eluted in 7 M urea, 0.1 M NaH₂PO₄/Na₂HPO₄, 0.01 M Tris/HCl, pH 7.0, 500 mM imidazole pH 7.0. For site-specific purification, we used the strategy developed previously^{10,13}.

Sample preparation and mass spectrometry

UFM1-enriched samples were supplemented with 1 M Tris-(2-carboxyethyl)-phosphine hydrochloride (TCEP) to a final concentration of 5 mM, and incubated for 20 minutes at room temperature. Iodoacetamide (IAA) was then added to the samples to a final concentration of 10 mM and samples were incubated in the dark for 15 minutes at room temperature. Lys-C and Trypsin digestions were performed according to the manufacturer's specifications. Lys-C was added in a 1:50 enzyme-to-protein ratio, samples were incubated at 37 °C for 4 hours, and subsequently 3 volumes of 100 mM Tris-HCl pH 8.5 were added to dilute urea to 2 M. Trypsin (V5111, Promega) was added in a 1:50 enzyme-to-protein ratio and samples were incubated overnight at 37 °C. For site-specific sample preparation, we used the strategy developed previously^{10,13}.

Then, digested samples were desalted, desalted samples were further concentrated on STAGE-tips as described previously^{10,13}. Samples were eluted with 0.1% formic acid in 80% acetonitrile. Elution step has been vacuum dried using a SpeedVac RC10.10 (Jouan, France) and before online nanoflow liquid chromatography-tandem mass spectrometry (nanoLC-MS/MS), final fractions were dissolved in 10 μL 0.1% formic acid.

Experiments were performed on a Q-Exactive Orbitrap (Thermo Fisher Scientific, Germany) connected with an EASY-nLC 1000 system (Proxeon, Odense, Denmark) through a nano-electrospray ion source. Peptides were separated in a 15 cm analytical column with an inner-diameter of 75 μm, in-house packed with 1.9AQ - μm C18 beads (ReproSpher-DE, Pur, Dr. Manish, Ammerbuch-Entringen, Germany).

The gradient length was 120 minutes from 2% to 95% acetonitrile in 0.1% formic acid at a flow rate of 200 nL/minute. The mass spectrometer was operated in a data-dependent acquisition mode with a top 10 method. Full-scan MS spectra were acquired at a target value of 3×10^6 and a resolution of 70,000, and the Higher-Collisional Dissociation (HCD) tandem mass spectra (MS/MS) were recorded at a target value of 1×10^5 and with a resolution of 17,500 with a normalized collision energy (NCE) of 25%. The maximum MS1 and MS2 injection times were 20 ms and 60 ms, respectively. The

precursor ion masses of scanned ions were dynamically excluded (DE) from MS/MS analysis for 60 sec. Ions with charge 1, and greater than 6 were excluded from triggering MS2 events.

For samples enriched for identification of UFM1 acceptor lysines, a 120-minute gradient was used for chromatography. Data dependent acquisition with a top 5 method was used. Maximum MS1 and MS2 injection times were 20 ms and 250 ms, respectively. Resolutions, normalized collision energy and automatic gain control target were set as mentioned previously. Dynamic exclusion was set to 20 sec.

Mass spec data analysis

Site level UFMylation data analysis

Site-specific purification was performed in three biological replicates, and all samples were measured in technical duplicates. All 18 RAW files were analyzed by MaxQuant (version 1.5.3.30). The first search was carried out with a mass accuracy of 20 ppm, while the main search used 64.5 ppm for precursor ions. Database searches were performed with Trypsin/P specificity, allowing three missed cleavages. Carbamidomethylation of cysteine residues was considered as a fixed modification. Mass tolerance of MS/MS spectra was set to 20 ppm to search against an in silico digested UniProt reference proteome for Homo sapiens (2017-30-01). Additionally, MS/MS data were searched against a list of 245 common mass spectrometry contaminants by Andromeda. Oxidation (M) and Acetyl (Protein N-term) were set as variable modifications. Additionally, VG modified lysine was introduced as a variable modification with a composition of $C_7H_{12}N_2O_2$ and a monoisotopic mass of 156.090 Da. Match between runs was used with 0.7 min match time window and 20 min alignment time window.

Interactors of Ufmylated RPL26

Protein lists generated by MaxQuant were further analyzed by Perseus (Version 1.5.5.3). Proteins identified only by site and as a common contaminant were filtered out, and then all the LFQ intensities were \log_2 transformed. Different experiments were annotated in to six group, HeLa-Flag, HeLa-Flag-RPL26, HeLa-His10-Ufm1-K0-Flag, HeLa-His10-Ufm1-K0-Flag-RPL26, HeLa-His10-Ufm1-K0-Flag (without UFSP2), HeLa-His10-Ufm1-K0-Flag-RPL26 (without UFSP2). Proteins identified in at least one treatment condition and found in at least three biological replicates were included for further analysis. For each experimental condition individually, missing values were imputed using Perseus software by normally distributed values with a 1.8 downshift (\log_2) and a randomized 0.3 width (\log_2). Final corrected P values were filtered to be less than 0.05. Then, average \log_2 ratios for HeLa-His10-Ufm1-K0-Flag-RPL26 vs HeLa-His10-Ufm1-K0-Flag were calculated and P values of each protein across all treatment conditions were calculated by T-tests. Proteins were selected as Ufmylated RPL26 interactors when their average \log_2 ratios are greater than 1 and corresponding p values were less than 0.05. Volcano plots to demonstrate identified proteins preferentially binding to UFMylated RPL26.

References

- 1 Deribe, Y. L., Pawson, T. & Dikic, I. Post-translational modifications in signal integration. *Nat Struct Mol Biol* **17**, 666-672, doi:10.1038/nsmb.1842 (2010).
- 2 Han, Z. J., Feng, Y. H., Gu, B. H., Li, Y. M. & Chen, H. The post-translational modification, SUMOylation, and cancer (Review). *Int J Oncol* **52**, 1081-1094, doi:10.3892/ijo.2018.4280 (2018).
- 3 Vertegaal, A. C. Uncovering ubiquitin and ubiquitin-like signaling networks. *Chem Rev* **111**, 7923-7940, doi:10.1021/cr200187e (2011).
- 4 Kerscher, O., Felberbaum, R. & Hochstrasser, M. Modification of proteins by ubiquitin and ubiquitin-like proteins. *Annu Rev Cell Dev Biol* **22**, 159-180, doi:10.1146/annurev.cellbio.22.010605.093503 (2006).
- 5 Choudhary, C. & Mann, M. Decoding signalling networks by mass spectrometry-based proteomics. *Nat Rev Mol Cell Biol* **11**, 427-439, doi:10.1038/nrm2900 (2010).
- 6 Schratzenholz, A., Klemm, M. & Cahill, M. Potential of comprehensive toxico-proteomics: quantitative and differential mining of functional proteomes from native samples. *Altern Lab Anim* **32 Suppl 1A**, 123-131 (2004).
- 7 Chen, Z., Zhou, Y., Zhang, Z. & Song, J. Towards more accurate prediction of ubiquitination sites: a comprehensive review of current methods, tools and features. *Brief Bioinform* **16**, 640-657, doi:10.1093/bib/bbu031 (2015).
- 8 Ghosh, S. & Dass, J. F. Study of pathway cross-talk interactions with NF-kappaB leading to its activation via ubiquitination or phosphorylation: A brief review. *Gene* **584**, 97-109, doi:10.1016/j.gene.2016.03.008 (2016).
- 9 Tsuchida, S., Satoh, M., Takiwaki, M. & Nomura, F. Ubiquitination in Periodontal Disease: A Review. *Int J Mol Sci* **18**, doi:10.3390/ijms18071476 (2017).
- 10 Hendriks, I. A. *et al.* Site-specific mapping of the human SUMO proteome reveals co-modification with phosphorylation. *Nat Struct Mol Biol* **24**, 325-336, doi:10.1038/nsmb.3366 (2017).
- 11 Hendriks, I. A. & Vertegaal, A. C. A high-yield double-purification proteomics strategy for the identification of SUMO sites. *Nat Protoc* **11**, 1630-1649, doi:10.1038/nprot.2016.082 (2016).
- 12 Xiao, Z. *et al.* System-wide Analysis of SUMOylation Dynamics in Response to Replication Stress Reveals Novel Small Ubiquitin-like Modified Target Proteins and Acceptor Lysines Relevant for Genome Stability. *Mol Cell Proteomics* **14**, 1419-1434, doi:10.1074/mcp.O114.044792 (2015).
- 13 Hendriks, I. A. *et al.* Uncovering global SUMOylation signaling networks in a site-specific manner. *Nat Struct Mol Biol* **21**, 927-936, doi:10.1038/nsmb.2890 (2014).
- 14 Munk, S. *et al.* Proteomics Reveals Global Regulation of Protein SUMOylation by ATM and ATR Kinases during Replication Stress. *Cell Rep* **21**, 546-558, doi:10.1016/j.celrep.2017.09.059 (2017).
- 15 Komatsu, M. *et al.* A novel protein-conjugating system for Ufm1, a ubiquitin-fold modifier. *EMBO J* **23**, 1977-1986, doi:10.1038/sj.emboj.7600205 (2004).
- 16 Kang, S. H. *et al.* Two novel ubiquitin-fold modifier 1 (Ufm1)-specific proteases, UfSP1 and UfSP2. *J Biol Chem* **282**, 5256-5262, doi:10.1074/jbc.M610590200 (2007).
- 17 Tatsumi, K. *et al.* A novel type of E3 ligase for the Ufm1 conjugation system. *J Biol Chem* **285**, 5417-5427, doi:10.1074/jbc.M109.036814 (2010).

- 18 Hertel, P. *et al.* The ubiquitin-fold modifier 1 (Ufm1) cascade of *Caenorhabditis elegans*. *J Biol Chem* **288**, 10661-10671, doi:10.1074/jbc.M113.458000 (2013).
- 19 Daniel, J. & Liebau, E. The ufm1 cascade. *Cells* **3**, 627-638, doi:10.3390/cells3020627 (2014).
- 20 Yoo, H. M. *et al.* Modification of ASC1 by UFM1 is crucial for ERalpha transactivation and breast cancer development. *Mol Cell* **56**, 261-274, doi:10.1016/j.molcel.2014.08.007 (2014).
- 21 Yoo, H. M., Park, J. H., Jeon, Y. J. & Chung, C. H. Ubiquitin-fold modifier 1 acts as a positive regulator of breast cancer. *Front Endocrinol (Lausanne)* **6**, 36, doi:10.3389/fendo.2015.00036 (2015).
- 22 Garrett, R. A. & Wittmann, H. G. Structure and function of the ribosome. *Endeavour* **32**, 8-14 (1973).
- 23 Henderson, E. *et al.* A new ribosome structure. *Science* **225**, 510-512 (1984).
- 24 Khatter, H., Myasnikov, A. G., Natchiar, S. K. & Klaholz, B. P. Structure of the human 80S ribosome. *Nature* **520**, 640-645, doi:10.1038/nature14427 (2015).
- 25 Petrov, A. S. *et al.* RNA-magnesium-protein interactions in large ribosomal subunit. *J Phys Chem B* **116**, 8113-8120, doi:10.1021/jp304723w (2012).
- 26 Wild, K., Rosendal, K. R. & Sinning, I. A structural step into the SRP cycle. *Mol Microbiol* **53**, 357-363, doi:10.1111/j.1365-2958.2004.04139.x (2004).
- 27 Simsek, D. *et al.* The Mammalian Ribo-interactome Reveals Ribosome Functional Diversity and Heterogeneity. *Cell* **169**, 1051-1065 e1018, doi:10.1016/j.cell.2017.05.022 (2017).
- 28 Pirone, L. *et al.* A comprehensive platform for the analysis of ubiquitin-like protein modifications using in vivo biotinylation. *Sci Rep* **7**, 40756, doi: 10.1038/srep40756 (2017).
- 29 Zhang, Y., Zhang, M., Wu, J., Lei, G. & Li, H. Transcriptional regulation of the Ufm1 conjugation system in response to disturbance of the endoplasmic reticulum homeostasis and inhibition of vesicle trafficking. *PLoS One* **7**, e48587, doi:10.1371/journal.pone.0048587 (2012).
- 30 Joassard, O. R. *et al.* Regulation of Akt-mTOR, ubiquitin-proteasome and autophagy-lysosome pathways in response to formoterol administration in rat skeletal muscle. *Int J Biochem Cell Biol* **45**, 2444-2455, doi:10.1016/j.biocel.2013.07.019 (2013).
- 31 Ishimura, R. *et al.* A novel approach to assess the ubiquitin-fold modifier 1-system in cells. *FEBS Lett* **591**, 196-204, doi:10.1002/1873-3468.12518 (2017).
- 32 Merbl, Y., Refour, P., Patel, H., Springer, M. & Kirschner, M. W. Profiling of ubiquitin-like modifications reveals features of mitotic control. *Cell* **152**, 1160-1172, doi:10.1016/j.cell.2013.02.007 (2013).
- 33 Zhang, Y. *et al.* Negative regulation of HDM2 to attenuate p53 degradation by ribosomal protein L26. *Nucleic Acids Res* **38**, 6544-6554, doi:10.1093/nar/gkq536 (2010).
- 34 Chen, J., Guo, K. & Kastan, M. B. Interactions of nucleolin and ribosomal protein L26 (RPL26) in translational control of human p53 mRNA. *J Biol Chem* **287**, 16467-16476, doi:10.1074/jbc.M112.349274 (2012).
- 35 Cai, Y. *et al.* UFBP1, a Key Component of the Ufm1 Conjugation System, Is Essential for Ufm1-Mediated Regulation of Erythroid Development. *PLoS Genet* **11**, e1005643, doi:10.1371/journal.pgen.1005643 (2015).
- 36 Singh, R. *et al.* Cryo-electron microscopic structure of SecA protein bound to the 70S ribosome. *J Biol Chem* **289**, 7190-7199, doi:10.1074/jbc.M113.506634 (2014).

- 37 Nierhaus, K. H. Nobel Prize for the elucidation of ribosome structure and insight into the translation mechanism. *Angew Chem Int Ed Engl* **48**, 9225-9228, doi:10.1002/anie.200905795 (2009).
- 38 Cisterna, B. & Biggiogera, M. Ribosome biogenesis: from structure to dynamics. *Int Rev Cell Mol Biol* **284**, 67-111, doi:10.1016/S1937-6448(10)84002-X (2010).
- 39 Dunkle, J. A. & Cate, J. H. Ribosome structure and dynamics during translocation and termination. *Annu Rev Biophys* **39**, 227-244, doi:10.1146/annurev.biophys.37.032807.125954 (2010).
- 40 Wilson, D. N. & Doudna Cate, J. H. The structure and function of the eukaryotic ribosome. *Cold Spring Harb Perspect Biol* **4**, doi:10.1101/cshperspect.a011536 (2012).
- 41 Morgan, D. G., Menetret, J. F., Neuhof, A., Rapoport, T. A. & Akey, C. W. Structure of the mammalian ribosome-channel complex at 17Å resolution. *J Mol Biol* **324**, 871-886 (2002).
- 42 Nakatogawa, H. & Ito, K. The ribosomal exit tunnel functions as a discriminating gate. *Cell* **108**, 629-636 (2002).
- 43 Menetret, J. F. *et al.* Ribosome binding of a single copy of the SecY complex: implications for protein translocation. *Mol Cell* **28**, 1083-1092, doi:10.1016/j.molcel.2007.10.034 (2007).
- 44 Roux, P. P. *et al.* RAS/ERK signaling promotes site-specific ribosomal protein S6 phosphorylation via RSK and stimulates cap-dependent translation. *J Biol Chem* **282**, 14056-14064, doi:10.1074/jbc.M700906200 (2007).
- 45 Grundy, M. *et al.* Early changes in rpS6 phosphorylation and BH3 profiling predict response to chemotherapy in AML cells. *PLoS One* **13**, e0196805, doi:10.1371/journal.pone.0196805 (2018).
- 46 Khalailieh, A. *et al.* Phosphorylation of ribosomal protein S6 attenuates DNA damage and tumor suppression during development of pancreatic cancer. *Cancer Res* **73**, 1811-1820, doi:10.1158/0008-5472.CAN-12-2014 (2013).
- 47 Spence, J. *et al.* Cell cycle-regulated modification of the ribosome by a variant multiubiquitin chain. *Cell* **102**, 67-76 (2000).
- 48 Higgins, R. *et al.* The Unfolded Protein Response Triggers Site-Specific Regulatory Ubiquitylation of 40S Ribosomal Proteins. *Mol Cell* **59**, 35-49, doi:10.1016/j.molcel.2015.04.026 (2015).
- 49 Kramer, G., Boehringer, D., Ban, N. & Bukau, B. The ribosome as a platform for co-translational processing, folding and targeting of newly synthesized proteins. *Nat Struct Mol Biol* **16**, 589-597, doi:10.1038/nsmb.1614 (2009).
- 50 Kobayashi, K. *et al.* Structure of a prehandover mammalian ribosomal SRP.SRP receptor targeting complex. *Science* **360**, 323-327, doi:10.1126/science.aar7924 (2018).
- 51 Vellinga, J. *et al.* A system for efficient generation of adenovirus protein IX-producing helper cell lines. *J Gene Med* **8**, 147-154, doi:10.1002/jgm.844 (2006).
- 52 Chevallet, M., Luche, S. & Rabilloud, T. Silver staining of proteins in polyacrylamide gels. *Nat Protoc* **1**, 1852-1858, doi:10.1038/nprot.2006.288 (2006).

